Iraqi National Journal of Earth Science, Vol. 26, No. 3, 2026(187-194)

Iraqi National Journal of Earth Science

www.earth.uomosul.edu.iq

Assessing Electrode Configuration Performance in Imaging Deep Concrete Piles Using 2D Electrical Resistivity Surveys

Raad Eissa[1*] **Falah H. Maziqa** [2] **Sany E. Hannina** [3]

raad.m@uokerbala.edu.iq falah_hasan@karbala.edu.iq sany.geargees@uobasrah.edu.iq

[1] *Department of Civil Engineering, College of Engineering, University of Kerbala, Karbala, Iraq.*
[2] *General Directorate of Education in Holy Karbala Province, Karbala, Iraq.*
[3] *Department of Geology, College of Science, University of Basrah, Basrah, Iraq.*

Received: 17 June 2025 Received in revised form: 18 July 2025 Accepted: 18 August 2025
Available online: 01 July 2026

Abstract

For rapid site investigation and buried foundation imaging, the electrical resistivity method is widely applied. This study concentrates on imaging a concrete pile foundation of 0.5 m in width and 200 Ohm.m of resistivity buried in a host background of 100 Ohm.m. The most popular electrode configurations are applied using different electrode spacing (0.1, 0.25, 0.5, and 1 m). Multiple data sets are numerically generated using the finite difference method and then inverted using the robust inversion algorithm constructed in the computer software RES2DINV. The obtained 2D resistivity images reveal the ability of dipole-dipole and equatorial dipole-dipole configurations in detecting the pile; the Wenner configuration shows less ability, and the gradient, multiple gradient, and pole-pole configurations are the poorest. In addition, most of the trialed configurations have detected the top part of the pile rather than the bottom. It is recommended, therefore, to apply high-resolution surveys using the dipole-dipole, equatorial dipole-dipole and the Wenner electrode configurations.

Keywords:

Brownfield site investigation, Buried concrete pile, ERT, Wenner configuration.

DOI: 10.33899/injes.v26i3.60340, ©Authors, 2026, College of Science, University of Mosul.

1. Introduction

The need for redevelopment of previously used sites increases the need to perform non-destructive techniques, such as geophysical methods, for imaging subsurface natural and man-made structures. The non-destructive site investigation techniques provide advantages over destructive techniques through cost, time (McCann et al., 1997), and more importantly, through the possibility of three-dimensional surveys. The geophysical surveys, including the electrical resistivity tomography (ERT) method, are globally utilized for geotechnical and environmental surveys (Reynolds, 2011; Shazly et al., 2023; Brahmi et al., 2023; Basri et al., 2024; Berhi and Al-Saadi, 2024; Abbas et al., 2025; Ahmed et al., 2025).

Electrical resistivity surveys are conducted by using what are called electrode configurations, which refer to the diversified order of the electrodes. Szalai and Szarka (2008) summarized more than 100 different electrode configurations that have been utilized in the ERT surveys. These configurations have certain advantages and limitations over each other; therefore, most of the ERT surveys have been conducted using more than one electrode configuration. Besides the real-case investigations, numerical modelling studies have been conducted to investigate the performance of different electrode configurations, and different buried foundations using 2D surveys (Martorana and Capizzi, 2023; Eissa, 2024a) and 3D surveys (Eissa, 2022a; Martorana and Capizzi, 2023). However, Eissa (2022b) stated that numerical modelling studies might have certain limitations and need to be confirmed by real-case data sets

Buried foundations, especially those for historical ancient buildings, are almost characterized by shallow and wide dimensions. In addition, it is built from different construction materials such as natural rock blocks, masonry, and others (Cardarelli et al., 2018; Giocoli et al., 2019). However, since the cement and concrete industry became a worldwide industry, shallow and deep foundations are almost constructed from concrete and reinforced concrete. Abu-Zeid et al. (2006) found that the resistivity response of the same buried foundation can be observed within a wide range of values due to its location to the groundwater table and groundwater chemistry and deterioration status; where the resistivity response of the same masonry brick foundation ranges from less than 10 Ωm to more than 150 Ωm. While different shallow foundations have been investigated throughout real-case or numerical modelling studies, deep foundations (i.e., piles) have not been investigated using the 2D ERT.

2. Aim of Study

Testing the performance of the 2D resistivity method for buried pile investigation is the purpose of this investigation. To achieve that purpose, the apparent resistivity datasets of a pile foundation buried in a homogeneous hosting background are generated using a numerical simulation approach. These created data sets are obtained using different electrode configurations; i.e., dipole-dipole (DD), Equatorial dipole-dipole (EDD), gradient (G), multiple gradient (MG), pole-pole (PP), and Wenner (W). Then, the data sets have been duplicated exerting different electrode spacing (i.e 0.1, 0.25, 0.5, and 1 m). After that, the generated data sets are processed to produce 2D images of the tested models through the inversion process by utilizing the RES2DINV software package. Finally, the performance of the applied electrode configurations and the electrode spacing is assessed by qualitative comparison.

3. Materials and Methods

This study is conducted using the numerical modelling approach RES2DMOD (ver. 3.01 Geotomo) to generate the apparent electrical resistivity readings of the investigated piles. The finite difference algorithm is performed through the modelling step (Loke and Barker, 1996). The most popular configuration types for buried foundations and geotechnical studies (i.e., Wenner, dipole-dipole, equatorial dipole-dipole, gradient, multiple gradient, and pole-pole configurations) are applied to generate the apparent resistivity readings. Different electrode spacing (i.e., 0.1, 0.25, 0.5, and 1 m) are utilized along with 151 electrodes to spread profiles of 15, 37.5, 75, and 150 m, respectively. Four nodes are chosen between any two adjacent electrodes (i.e., the cell size is half of the electrode spacing).

For all the duplicated configurations and electrode spacing, a buried foundation (a slender pile) having a square cross section of 0.5 m in the (x) and (y) directions is modelled and regarded as the target of the investigation. The buried pile is embedded in homogeneous media, i.e., soil (Fig. 1). The depth of the pile varies with the electrode spacing. Where the pile's depths are 3, 7.5, 15.5, and 21 m, with 0.1, 0.25, 0.5, and 1 m electrode spacing. These different depths are modelled in consideration of the expected maximum investigated depth of a certain length of each survey profile. The pile appears differently in Figure (1) due to the differences in depth and horizontal distance utilized by each survey profile.

Due to the wide range of buried concrete foundations' electrical response as documented by Arjwech et al. (2013) and Lysdahl et al. (2017). The investigated pile foundations are modelled with a resistivity value of 200 Ωm, and the hosting background is modelled with 100 Ωm; a thin topsoil layer was added with a resistivity value of 50 Ωm (Fig. 1).

The RES2DINV x64 (ver. 4.01 Geotomo software) used for data processing is utilized to process the generated readings, as other researchers (Hasan et al., 2021; Eissa, 2022 a, b) have utilized. A robust inversion algorithm is frequently applied to detect blocky anomalies of sharp changes with the hosting background; therefore, it is applied in the inversion process. Factors of 0.05 and 0.005 are applied as a robust data constraint cut-off factor and a robust model constraint cut-off factor, respectively. To mimic the ground heterogeneity, researchers have applied a certain level of noise to the generated resistivity datasets (e.g., Zhou and Dahlin, 2003, Abdullah et al., 2018). Eissa (2024 b) found a slight increase in the RMSE of inverted datasets with an added noise ratio up to 4%.

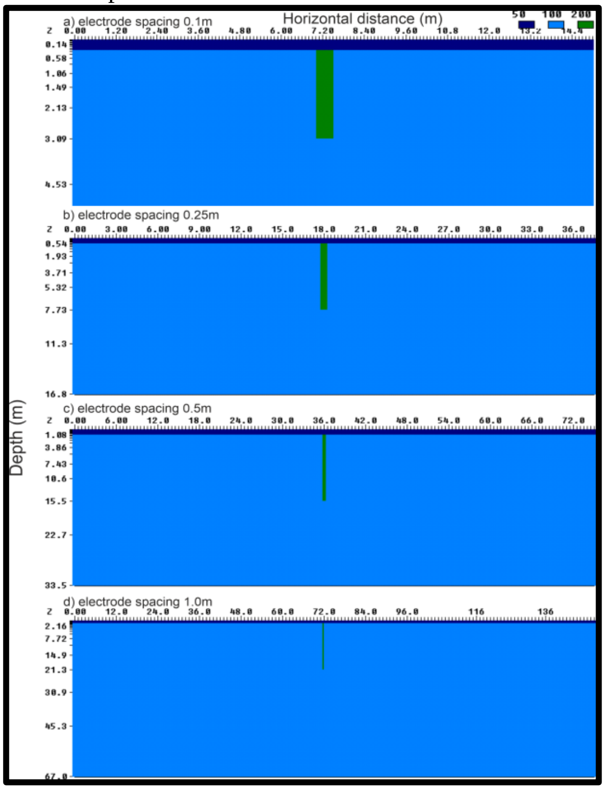

Fig. 1: Forward models of the tested buried pile, dark blue refers to the top soil layer (50 Ω.m), pale blue refers to the hosting ground (100 Ω.m), green indicates the investigated pile (200 Ω.m). Note: the piles have the same dimension, but it appears differently due to different represented depths and horizontal distances.

4. Results

All the generated datasets are inverted using the RES2DINV package, then presented as 2D resistivity models. The qualitative representation helps in qualitative comparison and determining the optimal electrode configuration and the electrode spacing for buried pile foundation investigations. The top thin soil layer is imaged through all the deployed configurations and most of the utilized electrode spacing; the smaller electrode spacing (i.e., 0.1 m), however, generates the best representation of the top soil layer, as illustrated in Figs. (2-5), due to the high resolution of the inverted data.

Figure (2) shows the inverted images of the 0.1 m electrode spacing. All the investigated electrode configurations are able to detect the pile; however, different performances were recognized. The dipole-dipole configuration, as imaged in Figure (2-a), represents the best detection of the pile, which is imaged with a noticeable difference in the resistivity response down to about 3 m. The configuration shows the low-resistivity background underneath the investigated pile, which adds more advantage to its performance.

The equatorial dipole-dipole and Wenner configurations (Fig. 2 b and f) show a noticeable contrast for the pile; however, a smaller portion of the top of the pile was imaged. The other configurations (i.e., the G, MG, and PP) are able to detect the buried pile, but their poor performance is noticeable (Fig. 2 c, d, and e). These configurations are not able to recognize the investigated pile as a high-resistivity anomaly, besides the poor reconstruction of the original dimensions of the target.

The obtained inverted images of the 0.25 m electrode spacing and all of the investigated electrode configurations are represented in Fig. 3. The dipole-dipole configuration shows the pile as a noticeable resistive anomaly down to about 3 m. The resistivity response of the pile continues down to about 7 m; however, with less resistivity contrast with the hosting background as seen in Figure (3a).

The equatorial dipole-dipole shows similar findings to those of the dipole-dipole configuration; however, a shallower detection of the pile occurred where the pile response is imaged down to less than 4 m (Fig. 3 b). The multiple gradient configuration (Fig. 3 d) and the Wenner configuration (Fig. 3 f) show less ability to determine the investigated pile. Where the pile is imaged by a smaller resistivity anomaly and by less contrast compared with the hosting background. The gradient configuration, as shown in Figure (3 c), and the pole-pole configuration, as represented in Fig. 3e, are the poorest electrode configurations. The poor performance of the pole-pole configuration might be related to the limited data resolution of the configuration.

Considering the 0.25 m electrode spacing, the dipole-dipole configuration reconstructs the pile with good agreement with the actual dimensions, followed closely by the equatorial dipole-dipole. The G, MG, PP, and W configurations show a restricted recognition of the pile's dimensions.

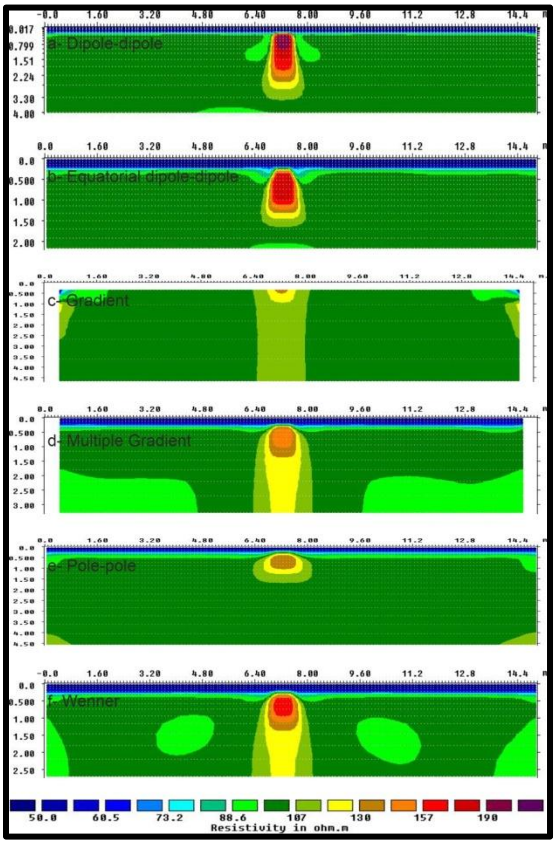

Fig. 2: 2D electrical resistivity response obtained from the investigated piles implementing 0.1m electrode spacing. The top horizontal blue represents the low-resistivity soil layer. The yellow to dark purple color contours at the center show the response from the pile. The rest, different green shades, show the hosting background.

Figure (4) represents the inverted images of the 0.5 m electrode spacing data sets for all the tested configurations. The dipole-dipole (Fig. 4 a) and the equatorial dipole-dipole (Fig. 4 b) configurations detect the target. The pile is determined with a higher resistivity value compared with the hosting media. The dipole-dipole is able to reconstruct the pile down to about 7 m; however, the equatorial dipole-dipole is able to reconstruct to less than 5 m. The other tested electrode configurations (G, MG, PP, and W) are able to detect a limited portion of the buried pile, which indicates the limited performance of these configurations (Fig. 4 c through f) using 0.5 m electrode spacing.

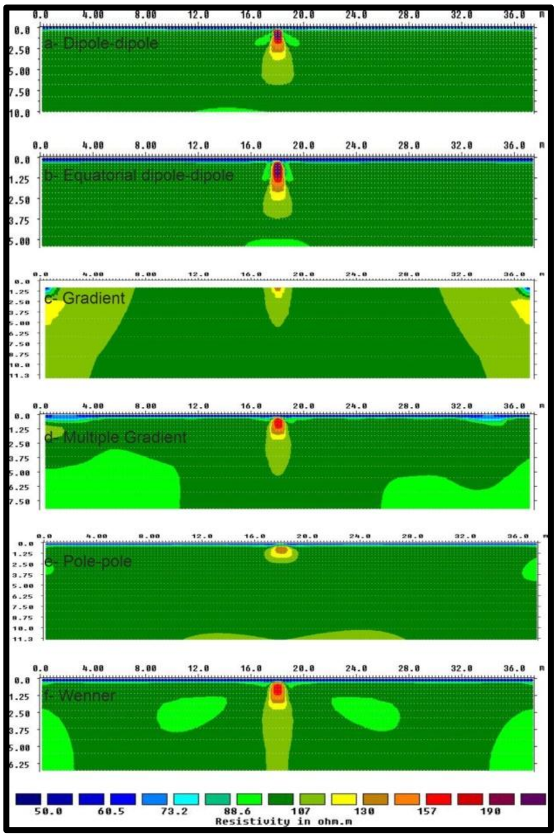

Fig. 3: 2D electrical resistivity response obtained from the investigated piles implementing 0.25m electrode spacing. The top horizontal blue represents the low-resistivity soil layer. The yellow to dark purple color contours at the center show the response from the pile. The rest, different green shades, show the hosting background.

Figure (5) shows the obtained inverted images using 1 m electrode spacing. The DD and EDD electrode configurations are able to detect the buried pile and reconstruct the pile down to about 10 m, which is about half of the total depth of the pile (Fig. 5 a and b). Whilst other electrode configurations (i.e., G, MG, PP, and W) recognize only a small portion of the top of the buried pile, which might be regarded as neglected detection and difficult to interpret (Fig. 5 c through f).

In Table 1, we summarize the qualitative performance of the tested electrode configurations. The summary shows a general decrease in the configuration performance with an increase in the electrode spacing.

Table 1: Ranking of the tested electrode configurations based on the qualitative findings. Solid black circle indicates good performance, solid gray circle indicates moderate performance, and open circle indicates poor performance.

Electrode configuration	Electrode spacing 0.1 m	Electrode spacing 0.25 m	Electrode spacing 0.5 m	Electrode spacing 1.0 m
Dipole-dipole	● (black)	● (black)	● (gray)	● (gray)
Equatorial dipole-dipole	● (black)	● (black)	● (gray)	● (gray)
Gradient	○	○	○	○
Multiple gradient	● (gray)	● (gray)	○	○
Pole-pole	○	○	○	○
Wenner	● (black)	● (gray)	○	○

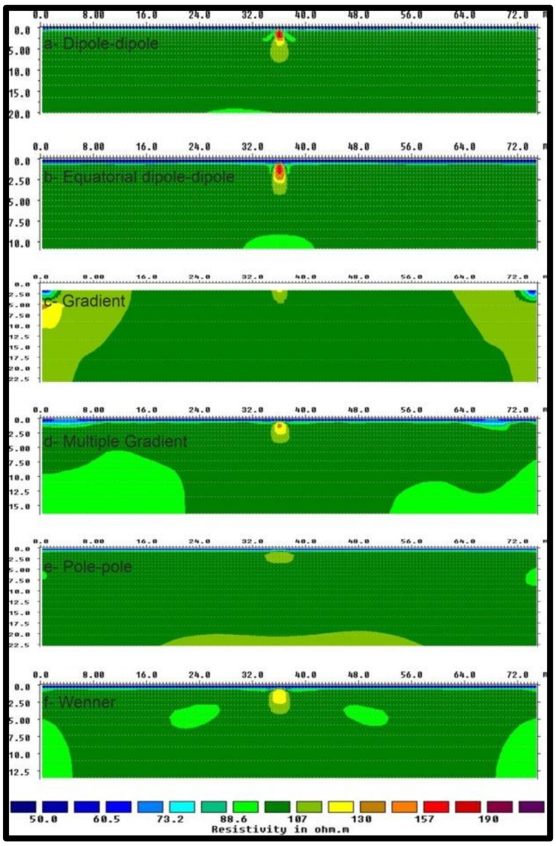

Fig. 4: 2D electrical resistivity response obtained from the investigated piles implementing 0.5m electrode spacing. The top horizontal blue represents the low-resistivity soil layer. The yellow to dark purple color contours at the center show the response from the pile. The rest, different green shades, show the hosting background.

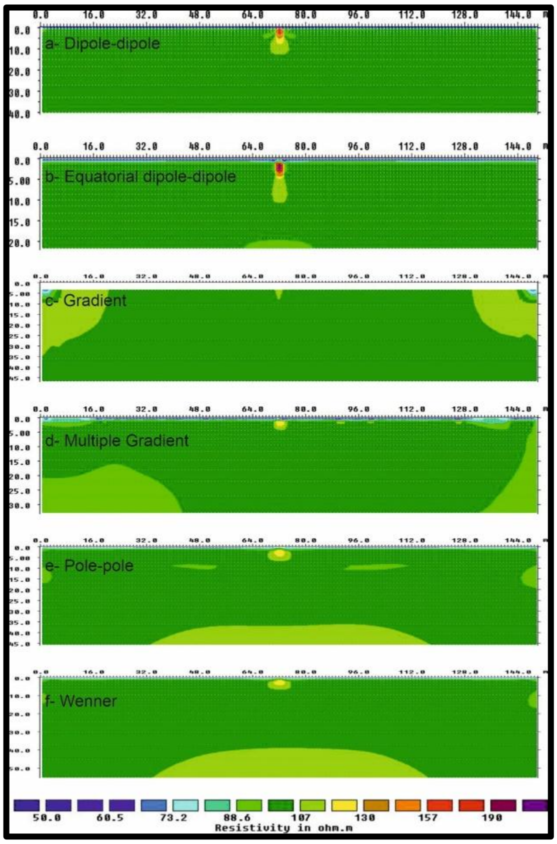

Fig. 5: 2D electrical resistivity response obtained from the investigated piles implementing 1m electrode spacing. The top horizontal blue represents the low-resistivity soil layer. The yellow to dark purple color contours at the center show the response from the pile. The rest, different green shades, show the hosting background.

5. Discussion

Two-dimensional electrical resistivity data sets are numerically modelled and created to simulate a buried concrete pile in a homogeneous hosting background as a potential target, especially in redevelopment brownfield sites (Reynolds, 2011). These data sets are generated using different electrode spacing (i.e., 0.1, 0.25, 0.5, and 1 m) and several popular electrode configurations. The dipole-dipole and equatorial dipole-dipole can detect the investigated pile position. The gradient, multiple gradient, and pole-pole configurations show limited detection.

The electrode spacing plays an important role in finding the investigated pile. The data sets generated by performing 0.1 m electrode spacing show the best performance, followed by the data sets generated using 0.25 m electrode spacing, which is interpreted due to the higher resolution of these data sets. However, performing survey profiles of 1m electrode spacing shows poor reconstruction of the pile regarding the pile dimensions of 0.5 m in x and y directions. This emphasizes the electrode spacing and pile dimensions and their slender shape relationship. Therefore, in field surveys, it is suggested to use electrode spacing smaller than the pile dimension to ensure the detectability of the pile.

Another limitation of the 1 m electrode spacing, as the largest spacing in this study, is highlighted due to the limited determination of the pile's total depth. The depth of the modelled pile is about 21 m; however, the imaged pile is down to about 10 m depth. This highlights the inherent limitation of the method and restricted reconstruction of the bottom parts of the pile (Reynolds, 2011). Ultimately, the possible erroneous interpretation of the obtained results.

This study has investigated certain site conditions (200 Ωm resistivity value of the pile and homogeneous hosting background), although 4 % noise is added during the forward modeling. Therefore, different resistivity values of the concrete pile and complex geology of the hosting background should be considered in real case scenarios. It should be pointed to the configurations with one or two remote electrodes, such as the pole-dipole and the pole-pole, might record a high level of noise.

Furthermore, performing other geophysical methods such as ground-penetrating radar (GPR) might help in joint interpretation and better foundation detection.

6. Conclusion

ERT survey profiles using different electrode spacing (0.1, 0.25, 0.5 and 1 m) and the most popular configurations are utilized to image a buried concrete pile foundation in a homogeneous background. The DD and EDD represent supreme performance; the Wenner shows moderate performance. However, the gradient, multiple gradient, and pole-pole configurations show a limited reconstruction of the pile.

Electrode spacing is identified as a crucial survey parameter considering the pile's dimensions, where shorter electrode spacing increases horizontal and vertical data resolution for the best imaging of the investigated pile.

Most of the configurations are capable of uncovering the pile's head but not the bottom. In addition, the deep part of the pile is most difficult to image, and an erroneous interpretation is possible. Therefore, prior data of the site is essential, and the obtained ERT data need to be attentively analyzed. In addition, this study is a preliminary model-based assessment and future work should include real case validation.

Furthermore, adopting the electrical resistivity method for foundation surveys, engineers and practitioners can contribute to numerical modeling using more than one configuration and high-resolution simulations to ensure the best resolution of the investigated site.

7. Acknowledgements

The authors are thankful to the anonymous reviewers for their time and efforts.

8. Conflict of Interest

The authors declare that they have no competing interests.

9. References

Abbas, S.S., Abed, A.M., and Al-Kubaisi, M.H.D., 2025. Integrating of 2D resistivity method and water quality index to evaluate groundwater in Ramadi city, Iraq. Iraqi National Journal of Earth Science, 25 (2), pp. 268-280. DOI: https://doi.org/10.33899/earth.2024.147946.1251.

Abdullah, F.M., Loke, M.H., Nawawi, M., and Abdullah, K., 2018. Assessing the reliability and performance of optimized and conventional resistivity arrays for shallow subsurface investigations. Journal of Applied Geophysics, 155, 237–245. https://doi.org/10.1016/j.jappgeo.2018.06.018

Abu-Zeid, N., Botteon, D., Cocco, G., and Santarato, G., 2006. Non-invasive characterisation of ancient foundations in Venice using the electrical resistivity imaging technique. NDT E Int. 39, 67–75. https://doi.org/10.1016/j.ndteint.2005.06.007

Ahmed, M.S., Al-Juraisy, B.A., Al-Mashhadany, A.Y., and Mutib, M., 2025. Using azimuthal resistivity survey technique to determining subsurface fractures of Quaternary deposits in the University of Mosul - Northern Iraq. Iraqi National Journal of Earth Science, 25 (1), pp. 34-49. https://doi.org/10.33899/earth.2024.146105.1219

Arjwech, R., Everett, M.E., Briaud, J.L., Hurlebaus, S., Medina-Cetina, Z., Tucker, S., and Yousefpour, N., 2013. Electrical resistivity imaging of unknown bridge foundations. Near Surface Geophysics, 11, pp. 591–598. https://doi.org/10.3997/1873-0604.2013023

Basri, M. El, Harmouzi, H., Basri, L. El, Mastere, M., Ouchen, I., Fellah, B. El, and Benzougagh, B., 2024. CBR Mapping Prediction from 2D Resistivity Imaging Using Regression Following Archie's Formula. Iraqi Geological Journal, 57, pp. 55–66. https://doi.org/10.46717/igj.57.1B.5ms-2024-2-14

Berhi, F.Z. and Al-Saadi, O.S., 2024. Electrical resistivity synthetic modeling and field survey for subsurface features investigation of the Borsippa archaeological site, Babylon governorate, Middle Iraq. Iraqi Geological Journal, 57, pp. 33–46. https://doi.org/10.46717/igj.57.1F.3ms-2024-6-12

Brahmi, S., Fehdi, C., Hadji, R., Brahmi, S., Hamad, A., and Hamed, Y., 2023. Karst-induced sinkhole detection using a tomography imaging survey, case of Setifian high plain, NE Algeria. Geotechnical and Geological Engineering, 41(3), pp. 1961-1976.

Cardarelli, E., De Donno, G., Oliveti, I., and Scatigno, C., 2018. Three-dimensional reconstruction of a masonry building through electrical and seismic tomography validated by biological analyses. Near Surface Geophysics, 16, pp. 53–65. https://doi.org/10.3997/1873-0604.2017040

Eissa, R., 2024a. The Practicality of Resistivity Method for Recognizing Vertically Distributed Anomalies Using Simulated Models. Iraqi Geological Journal, 57, pp. 204–213. https://doi.org/10.46717/igj.57.1B.16ms-2024-2-25

Eissa, R., 2024b. Noise Ratio Variation Effects on Visualizing Subsurface Targets in Electrical Resistivity Imaging (ERI) Sections. Iraqi Geological Journal, 57, pp. 262–273. https://doi.org/10.46717/igj.57.2F.17ms-2024-12-27

Eissa, R., 2022a. Identification of Different Shallow Foundations Using 3D Electrical Resistivity Modeling. Iraqi Geological Journal, 55, pp. 111–120. https://doi.org/10.46717/igj.55.2B.10Ms-2022-08-26

Eissa, R., 2022b. Pitfalls in Three-Dimensional Numerical Modeling of Electrical Resistivity Method. Iraqi Geological Journal, 55, pp. 144–156. https://doi.org/10.46717/igj.55.1C.11Ms-2022-03-30

Giocoli, A., Hailemikael, S., Bellanova, J., Calamita, G., Perrone, A., and Piscitelli, S., 2019. Site and building characterization of the Orvieto Cathedral (Umbria, Central Italy) by electrical resistivity tomography and single-station ambient vibration measurements. Engineering Geology, 260, 105195. https://doi.org/10.1016/j.enggeo.2019.105195

Hasan, M., Shang, Y., Meng, H., Shao, P., and Yi, X., 2021. Application of electrical resistivity tomography (ERT) for rock mass quality evaluation. Scientific Reports, 11, pp. 1–19. https://doi.org/10.1038/s41598-021-03217-8

Loke, M.H. and Barker, R.D., 1996. Rapid least-squares inversion of apparent resistivity pseudosections by a quasi-Newton method. Geophysical Prospecting, 44, pp. 131–152. https://doi.org/10.1111/j.1365-2478.1996.tb00142.x

Lysdahl, A.K., Bazin, S., Christensen, C., Ahrens, S., Günther, T., and Pfaffhuber, A.A., 2017. Comparison between 2D and 3D ERT inversion for engineering site investigations - A case study from Oslo Harbour. Near Surface Geophysics, 15, pp. 201–209. https://doi.org/10.3997/1873-0604.2016052

Martorana, R. and Capizzi, P., 2023. Evaluation of Artifacts and Misinterpretation in 2D Electrical Resistivity Tomography Caused by Three-Dimensional Resistive Structures of Regular or Irregular Shapes. Applied Science, 13. https://doi.org/10.3390/app13032015

McCann, D.M., Culshaw, M.G. and Fenning, P.J., 1997. Setting the standard for geophysical surveys in site investigation. Geological Society Engineering Geology Special Publication, 12, pp. 2–32. https://doi.org/10.1144/GSL.ENG.1997.012.01.01

Reynolds, J.M., 2011. An introduction to applied and environmental geophysics, second ed. Wiley-Blackwell, 696 P.

Shazly, T.F., Abd El Khafeef, A., Saleh, S.S., and Soliman, S.A., 2023. Utilizing shallow seismic refraction, electrical resistivity tomography, and ground penetrating radar techniques to evaluate geotechnical properties at El Galala Plateau, Gulf of Suez, Egypt. Iraqi National Journal of Earth Science, 23 (2), pp. 218-238. DOI: https://doi.org/10.33899/earth.2023.139838.1076

Szalai, S. and Szarka, L., 2008. On the classification of surface geoelectric arrays. Geophysical Prospecting, 56, pp. 159–175. https://doi.org/10.1111/j.1365-2478.2007.00673.x

Zhou, B. and Dahlin, T., 2003. Properties and effects of measurement errors on 2D resistivity imaging surveying. Near Surface Geophysics, 1, pp. 105–117. https://doi.org/10.3997/1873-0604.2003001

Iraqi National Journal of Earth Science, Vol. 26, No. 3, 2026(187-194)

Iraqi National Journal of Earth Science

www.earth.uomosul.edu.iq

تقييم أداء ترتيب الأقطاب الكهربائية في تصوير الركائز الخرسانية العميقة باستخدام مسوحات المقاومة الكهربائية ثنائية الأبعاد

رعد محمد عبدالزهره [1*] **فلاح حسن مزيقا** [2] **ساني أيليا جرجيس** [3]

raad.m@uokerbala.edu.iq falah_hasan@karbala.edu.iq sany.geargees@uobasrah.edu.iq

[1] قسم الهندسة المدنية، كلية الهندسة، جامعة كربلاء، كربلاء، العراق

[2] المديرية العامة للتربية في محافظة كربلاء المقدسة، كربلاء، العراق

[3] قسم علوم الأرض، كلية العلوم، جامعة البصرة، البصرة، العراق

تاريخ الاستلام: 17 حزيران 2025 تاريخ المراجعة: 18 تموز 2025 تاريخ القبول: 18 آب 2025

تاريخ النشر الالكتروني: 01 تموز 2026

الملخص

تُستخدم طريقة المقاومة النوعية الكهربائية على نطاق واسع في فحص المواقع بسرعة وتصوير الأساسات المدفونة. تركز هذه الدراسة على تصوير أساس خرساني بعرض 0.5 متر ومقاومته 200 أوم.متر مدفون في ارض مقاومتها الكهربائية 100 أوم.متر. طبق اكثر من ترتيب للاقطاب الكهربائية شيوعا وبمسافات مختلفة بين الأقطاب الكهربائية (0.1، 0.25، 0.5، و 1 متر). حيث تم توليد مجموعات من بيانات متعددة رقميًا باستخدام طريقة الفروق المحدودة (finite difference method)، ثم تمت معالجتها باستخدام خوارزمية الانعكاس القوية (robust inversion algorithm) المُصممة في البرنامج الحاسوبي (RES2DINV) لمعالجة وتحليل بيانات المقاومة الكهربائية. تُظهر صور المقاومة النوعية الكهربائية ثنائية الأبعاد التي تم الحصول عليها قدرة ترتيبات ثنائي القطب–ثنائي القطب وثنائي القطب–ثنائي القطب الاستوائي في اكتشاف الركائز الخرسانية، بينما يُظهر ترتيب Wenner قدرة أقل، وكانت ترتيبات التدرج ومتعددة التدرجات والقطب–القطب هي الأضعف. بالإضافة إلى ذلك، كشفت معظم الترتيبات التي تم اختبارها عن الجزء العلوي من الركائز الخرسانية المدفونة بدلاً من الجزء السفلي. لذلك، يُوصى بتطبيق مسوحات عالية الدقة من ترتيبات ثنائي القطب–ثنائي القطب وثنائي القطب–ثنائي القطب الاستوائي وترتيب Wenner.

الكلمات المفتاحية:

تحريات المواقع المستخدمة سابقا، الركائز الخرسانية المدفونة، طريقة المقاومة النوعية الكهربائية، ترتيب فنر.

DOI: 10.33899/injes.v26i3.60340, ©Authors, 2026, College of Science, University of Mosul.

===